Ann. Phys. (Leipzig) **10** (2001) 1–2, 9 – 18

# A single trapped atom: Light-matter interaction at the microscopic level

**V. Gomer and D. Meschede**

Institut für Angewandte Physik, Universität Bonn, Wegelerstr. 8, D–53115 Bonn
Germany
meschede@iap.uni-bonn.de

Received 18 Sep. 2000, accepted 6 Oct. 2000 by C. Thomsen

**Abstract.** For a single trapped atom the fluctuations of resonance fluorescence reveal its dynamic evolution at all relevant time scales. We review experimental results, extend interpretations and express expectations for future systems with fully controlled quantum properties.

**Keywords:** quantum physics, quantum optics, trapped atoms
**PACS:** 32.80 QK

*"Atome können wir nirgends wahrnehmen, sie sind wie alle Substanzen Gedankendinge"*
(Atoms themselves cannot be perceived anywhere, like all substances they are abstractions.)
Ernst Mach 1912

## 1 General

More than a century has elapsed since C.R.T. Wilson reported in 1897 [1] the first observation of traces of energetic charged particles in cloud chambers. Nevertheless single microscopic particles were considered of fictitious character long into the 20th century [2]. This notion was, however, changed when it became possible about two decades ago [3] to store and observe isolated Barium ions in an electromagnetic trap. Since then countless experiments have been carried out taking so called "Gedanken experiments" of quantum mechanics from conceptual ideas to experimental realization. In such experiments the resonance fluorescence of the trapped particles has served as an efficient detection method, and hence radiative interactions of ions and coherent light fields have been at the heart of such investigations. Since the advent of laser cooling [4] also neutral atoms can be trapped and observed in single quantities for long times [5–10] in analogy with ion traps. Experiments with individual ("single") neutral atoms are at the center of the present manuscript.

## 2 Experimenting with isolated neutral atoms

Experimental simplicity and robustness have made the magneto-optical trap [11] (MOT) (Fig. 1) the most widely used trap for neutral atoms and a universal source of cold

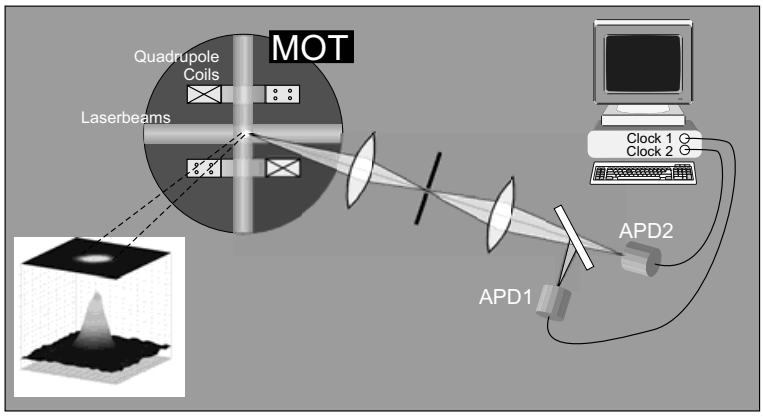


**Fig. 1** Experimental setup for the observation of single atoms in a magneto-optical trap (MOT). Camera picture shows spatial distribution of fluorescence of 6 Cesium atoms (resonance wavelength 852 nm). Photon arrival times are recorded in two channels.

atoms for experiments in many areas of physics. Atoms are stored at kinetic energies of order Doppler temperature $T_D = 125\,\mu$K or below. The observation of individual atoms in this device is facilitated by strong magnetic-field gradients [7] causing a strong localization of the atoms below 10 $\mu$m. For ultrahigh vacuum conditions storage times up to 10 minutes have been obtained, and the apparatus could be used for days at stable conditions.

Trapping as well as probe laser light is derived from stabilized diode lasers at 852 nm. For detection the resonance fluorescence from the trapped atoms is collected by a lens (0.5% solid angle), spatially filtered and imaged with a 50:50 beam splitter onto two 200 $\mu$m diameter avalanche photodiodes (APD). All photon arrival times are registered with resolution 50 ns. Thus all experiments can be analyzed *a posteriori* on a computer and at all time scales. We have obtained count rates up to 30 kHz per atom allowing shot noise limited detection. A step in the fluorescence count rate is associated with the arrival and departure of atoms (Fig. 2), and secure detection of the present number of atoms (up to 20) in the trap is possible in less than 10 ms.

## 3 Photon correlations and atomic dynamics

For many atoms the intensity of resonance fluorescence is associated with an average excitation of the atom. Fluctuations of the fluorescence intensity carry information on atomic variables such as excitation or magnetic orientation and reflect distortions from atomic equilibrium. Fluorescence quantum noise can be analyzed by means of the normalized intensity correlation function $g^{(2)}_{\alpha,\beta}(\tau)$ of electromagnetic fields $\alpha, \beta$ [12,13]. For classical fields with a time dependent intensity $I_\alpha(t)$ it is calculated from

$$g^{(2)}(\tau) = \frac{\langle I_\alpha(t) I_\beta(t+\tau)\rangle}{\langle I_\alpha(t)\rangle\langle I_\beta(t)\rangle} = \frac{\langle :\hat{n}_\alpha(t)\hat{n}_\beta(t+\tau):\rangle}{\langle \hat{n}_\alpha(t)\rangle\langle \hat{n}_\beta(t)\rangle} \quad . \tag{1}$$

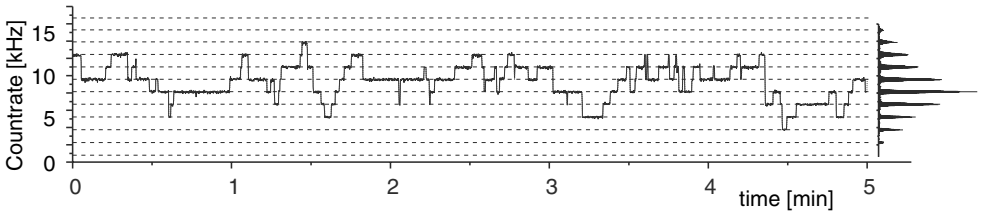


**Fig. 2** Time chart clip of atomic resonance fluorescence. Well resolved equidistant fluorescence levels correpond to integer numbers of atoms. Right: Distribution of count rates shows shot noise limited detection, here for an average of 5 atoms.

In quantum physics intensities are replaced by photon number operators $\hat{n}_\alpha(t)$ where : denotes normal ordering. In classical physics the autocorrelation function ($\alpha = \beta$) reduces to the variance of the field for $\tau = 0$ and hence must obey $g^{(2)}(\tau = 0) \geq 1$. Quantum properties of the electromagnetic field are signaled by $g^{(2)}(0) \leq 1$.

In an intuitive interpretation of second order photon correlations [13] it is said that the first observed photon prepares ("projects") the observed system onto a certain quantum (or also classical) state while the probablity to observe a second photon carries information about the relaxation dynamics. This interpretation is close to another method of analyzing microscopic dynamics subject to quantum fluctuations offered by the Monte Carlo wavefunction method [14]. In this numerical method the projection of the system under observation is explicitly accounted for by stochastic collapse of the corresponding wavefunction.

In summary, continuous observation of fluctuations in resonance fluorescence at constant experimental conditions allows to derive information about all atomic degrees of freedom leaving a signature on radiative properties. As an introduction we elucidate the well known phenomenon of photon antibunching for a single atom trapped in a MOT and subsequently extend this method to other atomic variables.

### *3.1 Nanosecond quantum fluctuations: Antibunching with trapped neutral atoms*

Resonance fluorescence has been a celebrated manifestation of nonclassical properties of light due to the observation of the so called phenomenon of photon antibunching with $g^{(2)}(0) = 0$: Detection of a photon prepares the radiating atom in its ground state, and subsequent emission of a second photon is delayed until the atom is reexcited. Initial experiments were carried out with very dilute beams of atoms [15,16], and more precise investigations became possible when ion traps were employed to achieve long-term confinement of a single atomic particle [17]. Antibunching is also present for an atom stored in a MOT driven by trapping laser light, as detailed in Fig. 3. A simple two-level model (solid lines) shows surprisingly good agreement with the experimental data even though up to 27 transitions may contribute with different coupling strengths. The enhanced probability at the first maximum can be attributed to the fact that the atom-light coupling undergoes variations due to motion in the trapping laser interference field as well as due to modifications of the magnetic sublevels.

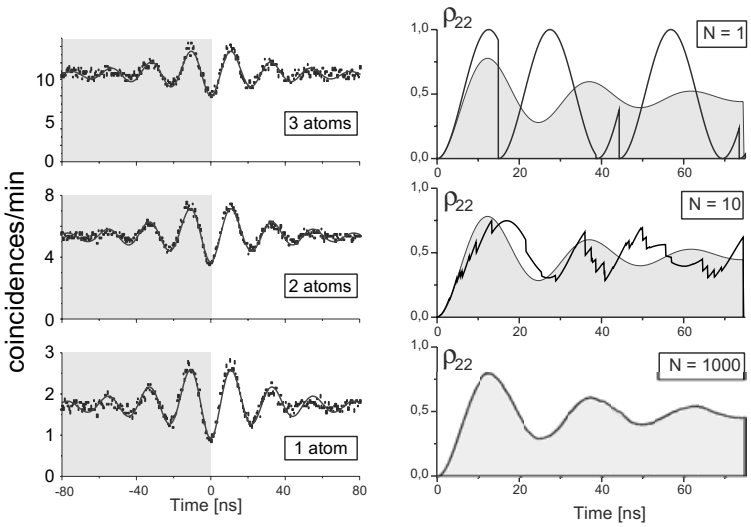


**Fig. 3** Left: Two photon correlation in the resonance fluorescence of 1, 2, and 3 Cesium atoms trapped in a MOT. The symmetric appearance of the signal is due to the fact that the "first" photon selects its channel at random. For 1 atom random events contribute 50% of the signal. The contrast is clearly reduced with increasing number of trapped atoms. Right: Numerical simulation of Rabi oscillations by the quantum Monte Carlo method for a single atom, adapted from [4]. The analytic result is shaded.

The right side of Fig. 3 shows a Monte Carlo simulation of coherent atomic evolution disturbed by random spontaneous emission. Averaging over many trajectories reproduces the density matrix calculation (shaded).

### *3.2 Microseconds: Bistable polarization of an atom*

Another interesting example of resolved quantum fluctuations can be found at microsecond time scale if the polarized fluorescence of a single atom is detected. The main theoretical assumption so far has been an ideal atom with only two energy levels, and it was surprisingly successful for the interpretation of nanoscale fluctuations. However, already for the MOT itself optical pumping between sublevels of a real atom is very important. An interplay between the complicated interference pattern of a laser field and multi-level atoms gives rise to many fascinating and subtle effects in laser cooling of neutral atoms such as sub-Doppler cooling and optical lattices [4].

In one dimension two counter propagating circularly polarized laser beams with the same handedness ($\sigma^+\sigma^-$ configuration) produce a light field with linear polarization everywhere. A threedimensional analogue is obtained for a variant of the MOT with a special configuration of light fields with full phase control [21–23]. The 1d-configuration is nevertheless a reasonable model for 3d since an atom diffusing through this field is essentially subject to a linear polarization which changes direction by a

full turn every wavelength and in every direction.

It is intuitively clear that a linearly driven classical emitter will continue to radiate with identical linear polarization until its direction is changed as a consequence of motion through the light field. It is straightforward to show [10] that for diffusive motion in a potential-free space strong correlations exist between vertical and horizontal linear components of the radiation field, $g^{(2)}_{vv}(\tau) = g^{(2)}_{hh}(\tau) = 1 + e^{-k^2\xi^2(\tau)}/2$ and $g^{(2)}_{vh}(\tau) = 2 - g^{(2)}_{vv}(\tau)$. [$\xi(t)$ describes the temporal spread of the atomic positional probability.] In contrast, left- and righthanded circular components do not show any correlations in this model, $g^{(2)}_{\ell\ell}(\tau) = g^{(2)}_{\ell r}(\tau) = 1$. Thus the classical model predicts strong correlations between orthogonal linear polarization components and no correlations between circular components in striking contradiction with experimental results (Fig. 4):

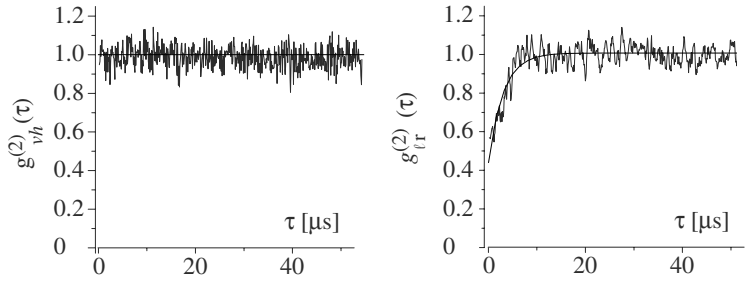


**Fig. 4** Measured photon correlations from a single atom in the linear polarized MOT field. Left: Correlation function $g^{(2)}_{vh}(\tau)$ for orthogonal linear polarization components. Right: Correlation function $g^{(2)}_{\ell r}(\tau)$ for orthogonal circular polarization components. Solid line: exponential fit.

Within our experimental uncertainties correlations are completely absent for linear polarization components of the fluorescence. The circular correlation contrast reaches values up to 62% indicating strong fluctuations of the atomic orientation.

Figure 5 shows a Monte-Carlo simulation of quantum trajectories for the $m_F$ Zeeman sublevels of the ground state $F = 4$ of Cs subject to linear polarization. The atom changes its quantum number due to absorption and emission of light and emits photons of all polarizations. As expected the averaged population distribution over all Zeeman sublevels is symmetric and does not show any orientation ($\langle m_F \rangle = 0$). For the dominant $m_F$-levels photons with horizontal and vertical polarization are emitted with nearly equal probability and hence correlations are suppressed.

A most interesting situation arises for correlations measured between circular polarization components. The quantization axes in this case is parallel to the direction of propagation and the local light field consists of equal parts of both orthogonal circular polarizations only. The corresponding $m_F$ population distribution is obtained from the preceding case by rotation of the density matrix by 90°. Again the $m_F$ distribution is symmetric around $m_F = 0$: In a linearly polarized field magnetic orientation of an atomic ensemble vanishes.

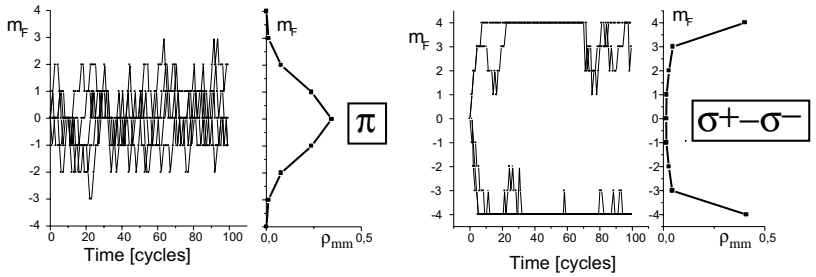


**Fig. 5** Left: Evolution of the Zeeman sublevel population in a Cs atom ($F = 4$) driven by linearly polarized light and with linearly polarized detection. All five trajectories start in the $m_F = 0$ state. Averaged population distribution to the right. Right: The same, but for the case of circularly polarized detection.

For an *individual* atom, however, this symmetry can be spontaneously broken by emission of a single circularly polarized photon. It projects the atom into its ground state, breaks the symmetry of the Zeeman substate population [18], and creates an imbalance in the interaction strengths with both circular polarization components. The next absorption will preferentially further enhance the asymmetry. The imbalance in the interaction strengths rapidly grows with $m_F$ leading to fast pumping into one of the outmost Zeeman states $m_F = \pm F$. The ratio of the interaction strengths in these stretched states reaches the value $(2F + 1)(F + 1)$ making them very stable for large $F$. Hence the atom in this oriented state prefers to radiate into the same polarization state as the first detected photon, resulting in anticoincidences in the cross correlation for orthogonal circular polarizations.

In the simulation in Fig. 5 we have artificially decoupled atomic internal and external degrees of freedom. While radiation pressure forces are balanced for an aligned atom with $\langle m_F \rangle$=0, they are unbalanced for an oriented atom since the local linearly polarized light field is created by *counterpropagating* laser beams with orthogonal circular polarizations. The imbalance in the light forces created by atomic orientation thus causes acceleration, or heating which is again damped by the usual laser friction forces [19]. Thus for our experiment we must acknowledge that the observation of a circularly polarized photon not only redefines atomic orientation but also its mechanical status: Internal and external atomic degrees of freedom are inextricably entangled. In a more detailed investigation we have measured that the correlation relaxation rate is indeed proportional to the average atomic velocity [23]. This indicates that relaxation of the bistable atomic magnetization is caused by atomic motion through the light field.

### *3.3 Milliseconds: Trap motion of an atom*

All correlations due to internal atomic dynamics have seized at the ms time scale. Another fluctuation can be generated through spatial resolution of resonance fluorescence. Since our experimental resolution is insufficient to fully resolve atomic trajectories at

the $\mu$m level we have split the intermediate image into two equal parts (left and right in Fig. 6) which were directed onto the two photon detectors. The result with strong correlations is also shown.

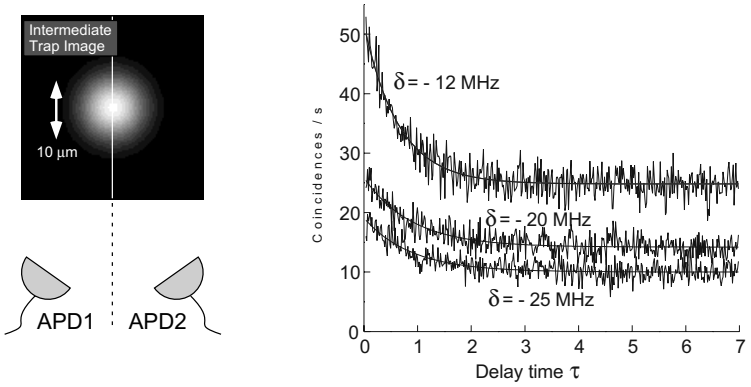


**Fig. 6** Two photon correlation caused by diffusive atomic motion in the trap. Left: Intermediate trap image is divided into two "states" which are directed to separate photon counters. Right: Correlation measurement. The relaxation time increases with laser detuning indicating decreasing atomic velocity.

We suggest an interpretation along the lines used before: Registration of a first photon projects the atom into one of the two halves of the trap volume, in close analogy to the atomic two level quantum system, but now for a classical probability distribution function. Fluorescence bursts are started and stopped through arrival and departure of an atom in the corresponding trap volume. On average one half of the fluorescence should originate in each of the halves, and we expect $g^{(2)}(0) > 1$.

A detailed analysis [10] shows that the shape of the correlation function can be understood from a Fokker-Planck equation describing diffusion in the trap. Evaluation of the positional damping time as a function of trap parameters such as laser detuning shows very good agreement with temperature measurements carried out with many atoms. Again the single atom resonance fluorescence method allows to derive this information in a non-invasive manner from "natural" disturbances of the system.

### *3.4 Seconds and minutes: Cold collisions*

Changes of the atom number in our trap represent the slowest dynamical rate in the system. In Fig. 7 we show isolated loading and loss events where two-atom losses due to inelastic two-body collisions can be unambiguously identified. At first sight it may indeed seem to be surprising that two or three atoms only stored in a volume of $(10\mu\text{m})^3$ collide so frequently. The reason for that is the presence of near-resonant laser light.

It is well known that interaction of two neutral atoms at large separations varies as the inverse sixth power of the interatomic distance, $\propto 1/R^6$, corresponding to

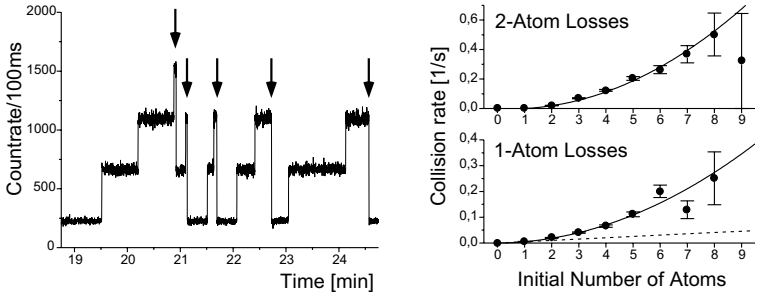


**Fig. 7** Left: Clip from typical MOT fluorescence signal. Five isolated cold collisions (two-atom losses) are shown (arrows). Right: Collisional loss rates as a function of initial atom number. 1-atom loss rate shows unexpected quadratic behaviour.

the potential of the familiar van der Waals forces [24]. However, in a MOT a significant fraction of atoms is excited, and the resonance dipole-dipole force proportional to $1/R^3$ arises [25]. The van der Waals forces with dipole-dipole interaction $H' = e^2/4\pi\epsilon_0(x_1x_2 + y_1y_2 - 2z_1z_2)/R^3 + \ldots$ are textbook examples of pure quantum interactions, and they can be used to derive quasimolecular potentials (Fig. 8) which dominate the processes governing cold collisions. The typical strengths of the interaction can be estimated from the square of the dipole moment $d$ which is associated with dipole transition $S \leftrightarrow P$ with corresponding natural linewidth $\Gamma = 2\omega_0^3 d^2/(3\epsilon_0 hc^3)$. The longest range potential in the problem of collisions between laser-cooled atoms is clearly the $R^{-3}$ potential for $S+P$ states given by $U = \pm\hbar\Gamma\left[R/(\lambda/2\pi)\right]^{-3}$, and it is of the order of Doppler temperature near the characteristic distance $\lambda/2\pi(\approx 136$ nm for Cs atoms). In this long-range region the ground-state curves connected to the $S+S$ asymptote are essentially flat. A laser detuned by $\Delta$ from resonance excites atom pairs to an attractive (for red detuning, $\Delta < 0$) or repulsive (for $\Delta > 0$) quasimolecular state, preferentially at the Condon distance $R_c$ given by $R_c^3 = C_3/\hbar|\Delta|$.

Three main exoergic collisional processes in MOT's [26] can be identified (Fig. 8): Fine-structure-changing collisions (FCC) are represented by $A+A+\hbar\omega \rightarrow A_2^*(P_{3/2}) \rightarrow A^*(P_{1/2})+A+\Delta E_{FCC}$ with energy $\Delta E_{FCC}/2$ transferred to each atom. For radiative escape (RE), a photon red-shifted from resonance is spontaneously emitted during the collision. The process is described by $A+A+\hbar\omega \rightarrow A_2^* \rightarrow A+A+\hbar\omega'$ with energy $\hbar(\omega-\omega')/2$ transferred to each atom. Exoergic hyperfine-changing collisions (HCC) on the molecular ground-state also lead to losses if the trap is sufficiently shallow.

Cold collisison experiments are usually associated with high atomic densities and as a consequence large numbers of trapped atoms. The main method of observing collisions has been to abruptly change experimental parameters (usually switching off or on an atomic beam loading the trap) and to watch the trap population decay or increase [26]. The observation of cold collisions with very few atoms provides unambiguous identifcation of collisional events including additional information. For example, we have found that a substantial fraction (up to 10 %) of cold collisional events result in the loss of one atom only [28]. This surprising and unresolved effect is principally

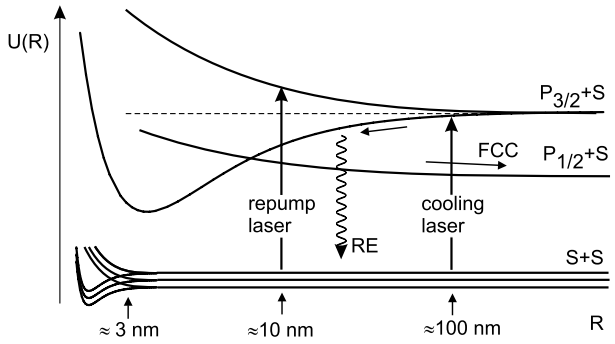


**Fig. 8** Schematic overview of collisional processes in a MOT (here for Cs atoms as example). Shown are interaction energies between two atoms in different states as a function of the internuclear distance R. Characteristic distances of resonant excitation by both MOT lasers are determined by the corresponding laser detunings: $\Delta \approx 1 - 4\Gamma$ or $\approx +2000\Gamma$ for cooling or repumping laser, respectively. Two possible light-induced exoergic collisional processes, FCC and RE are shown (see text). At very short distances a change of the ground state hyperfine structure can occur.

unobservable in experiments on many atoms. We have also observed a strong optical suppression of ground-state hyperfine-changing collisions in the trap by its repump laser field. The method can also remove potential ambiguities in experiments where an extra probe laser is introduced [27] in order to 'catalyse' different collisional loss channels. Such laser fields can strongly affect the performance of the trap [29], and it is in general difficult to clearly discriminate between changed excitation conditions and changes in the atom number, both modifying the total fluorescence signal. It is also easy to generalize the method for studies of heteronuclear collisions [30] where fluorescence from different species can easily be spectrally distinguished. One can furthermore speculate about the possibility to observe the formation of an individual molecule starting from two atoms.

## 4 Conclusion: Controlling the dynamics of individual neutral atoms

A single atom can be studied sensitively and at all time scales in a MOT. Quantum coherence is strongly inhibited by spontaneous emission in this trap, however. We have thus employed far off resonance optical dipole traps for single atoms and observed both long storage times as well as slow relaxation of quantum state population [31]. State-selective detection at the level of a single atom and deterministic preparation of a number of atoms on demand have been demonstrated. For example it is conceivable to improve recent single atom cavity QED experiments [32, 33] by introducing a desired number of atoms by means of the "optical tweezer" derived from the dipole trap. Together with recently demonstrated non-classical motional states of atoms [34] this system may ultimately offer an alternative for rivaling stored ion-systems.

**Acknowledgements**

Over the years many young physicists have intensely contributed to this work: K. Dästner, D. Frese, D. Haubrich, S. Knappe, S. Kuhr, A. Rauschenbeutel, H. Schadwinkel, D. Schrader, F. Strauch, B. Ueberholz, R. Wynands. We have received support from the Deutsche Forschungsgemeinschaft and the state of Nordrhein-Westfalen.

**References**

[1] C. R. T. Wilson, Philos. Trans. R. Soc. London **189** (1897) 265
[2] E. Mach, *Mechanik in ihrer Entwicklung*, Wiss. Buchges., Leipzig 1912
[3] W. Neuhauser, M. Hohenstatt, P. Toschek, H. Dehmelt Phys. Rev. A **22** (1980) 1137
[4] H. Metcalf and P. van der Straaten, *Laser cooling and trapping*, Springer, New York 1999
[5] Z. Hu and H. J. Kimble, Optics Lett. **19** (1994) 1888
[6] F. Ruschewitz, D. Bettermann, J. L. Peng, W. Ertmer, Europhys. Lett. **34** (1996) 651
[7] D. Haubrich, H. Schadwinkel, F. Strauch, B. Ueberholz, R. Wynands, D. Meschede Europhys. Lett. **34** (1996) 663-668
[8] P. A. Willems *et al.*, Phys. Rev. Lett. **78** (9) (1997) 1660
[9] V. Gomer, F. Strauch, B. Ueberholz, S. Knappe, D. Meschede, Phys. Rev. A **58** (1998) R1657
[10] V. Gomer, F. Strauch, B. Ueberholz, S. Knappe, D. Frese, D. Meschede, Appl. Phys. B **67** (1998) 689
[11] E. L. Raab, M. Prentiss, A. Cable, S. Chu, D. Pritchard Phys. Rev. Lett. **59** (1987) 2631
[12] R. J. Glauber Phys. Rev. **130** (1963) 2529, ibid. **131** (1963) 2766
[13] D. F. Walls and G. J. Milburn, *Quantum Optics*, Springer, New York 1994, p. 222
[14] K. Molmer, Y. Castin, J. Dalibard J. Opt. Soc. Am. B **10** (1993) 524-538
[15] H. J. Kimble, M. Dagenais, L. Mandel, Phys. Rev. Lett. **39** (1977) 691
[16] F.-M. Rateike, G. Leuchs, and H. Walther, results cited by J. D. Cresser, J. Häger, G. Leuchs, F.-M. Rateike, and H. Walther, in *Dissipative Systems in Quantum Optics*, R. Bonifatio, Ed., Topics in Current Physics, vol. 27, p. 21., Springer, Berlin 1982
[17] F. Diedrich and H. Walther, Phys. Rev. Lett. **58** (1987) 203
[18] W. M. Klipstein, S. K. Lamoreaux, E. N. Fortson , Phys. Rev. Lett. **76** (1996) 2266
[19] J. Dalibard, C. Cohen-Tannoudjii, J. Opt. Soc. Am. B **6** (1989) 2058
[20] C. Cohen-Tannoudji, in: J. Dalibard, J.-M. Raimond und J. Zinn-Justin (eds.), *Fundamental Systems in Quantum Optics*, 1, (North-Holland, Amsterdam, 1992)
[21] A. Rauschenbeutel, H. Schadwinkel, V. Gomer, D. Meschede, Optics Commun. **148** (1997) 45.
[22] H. Schadwinkel, U. Reiter, V. Gomer, D. Meschede, Phys. Rev. A **61** (2000) 13409
[23] H. Schadwinkel, U. Reiter, B. Ueberholz, V. Gomer, D. Meschede, IEEE J. Quantum Electronics **36** (2000) 36.
[24] H. Morgenau, Rev. Mod. Phys. **11** (1939) 1
[25] R. Eisenschitz and F. London, Z. Physik **60** (1930) 491
[26] P. S. Julienne, A. M. Smith, K. Burnett, in *Advances in Atomic, Molecular and Optical Physics* **30** (1993) 141, J. Weiner *et al.*, Rev. Mod. Phys. **71** (1999) 1
[27] D. Sesko *et al.*, Phys. Rev. Lett. **63** (1989) 961
[28] B. Ueberholz, , S. Kuhr, D. Frese, D. Meschede, V. Gomer, J. Phys. B: At. Mol. Opt. Phys. B **33** (2000) L135
[29] P. Feng *et al.*, Phys. Rev. A **47** (1993) R3495
[30] G. D. Telles *et al.*, Phys. Rev. A **59** (1999) R23
[31] D. Frese, S. Kuhr, B. Ueberholz, V. Gomer, D. Meschede, Phys. Rev. Lett. **85** (2000) 3777
[32] P. W. H. Pinkse, T. Fischer, P. Maunz, G. Rempe, Nature **404** (2000) 365
[33] C. J. Hood, T. W. Lynn, A. C. Doherty, A. S. Parkins, H. J. Kimble, Science **287** (2000) 1447
[34] M. Morinaga, I. Bouchoule, J.-C. Karam, and C. Salomon, Phys. Rev. Lett. **83** (2000) 4037